COMPUTERS IN PHYSICS

SEP/OCT 1992

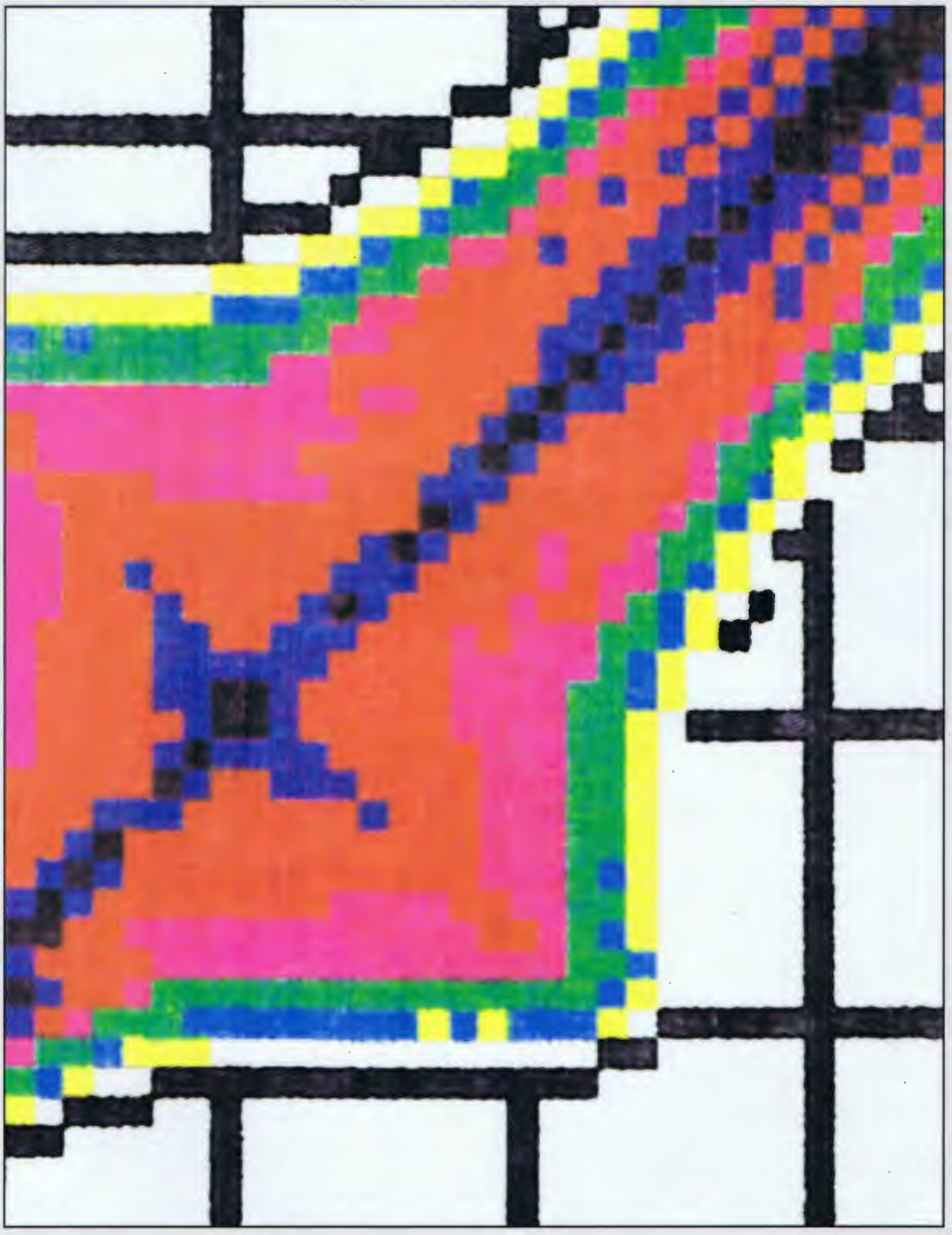

Visualizing Quantum Resonances

AMERICAN INSTITUTE OF PHYSICS

Object-Oriented Programming

COMPUTERS IN PHYSICS

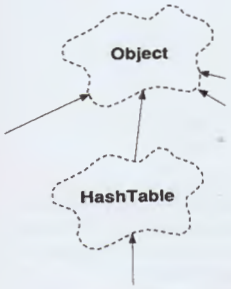

C++ Programming Language...450

```
feature specification
    ring: BITS 32 -- point
    BPM: BPMS -- BPM
    STRMAG: STRMAC
    NoCelem: INTEGER
            -- # of cell
    fitTune (nux: DOUBI
            -- Fit betatr
    Tune (dir: INTEGER
            -- Get betat
            -- dir=0 for
    setCODeps (eps: DO
            -- Set COD
    setCOD (dp: DOUBI
```

C Routines in Eiffel...456

Chemical Reaction Kinetics...494

COVER: Energy spreading versus initial energy, with color representing probability, reveals nonlinear resonance in Hilbert space of extreme Stark hydrogen. Paper begins on p. 483.

Contents

COMPUTERS IN PHYSICS (ISSN 0894–1866 coden CPHYE2) volume 6 number 5. Published bimonthly (6 issues per year) by the American Institute of Physics, 500 Sunnyside Blvd., Woodbury, NY 11797. Member subscription rates: $35.00 per year; foreign, $45.00; air freight to Europe, Asia and rest of Eastern Hemisphere, $55.00. Nonmember Individual subscription rates: United States and possessions, $45.00 per year; Canada, Mexico and rest of Western Hemisphere, $55.00; air freight to Europe, Middle East, North Africa, Asia and rest of Eastern Hemisphere, $65.00 per year. Nonmember Institutional subscription rates: United States and possessions, $195.00 per year; Canada, Mexico and rest of Western Hemisphere, $205.00; air freight to Europe, Middle East, North Africa, Asia and rest of Eastern Hemisphere, $215.00 per year. Back numbers, single copies, $35.00. Second Class Postage Paid at Woodbury, New York, and at additional mailing offices. POSTMASTER: Send address changes to Computers in Physics Subscription Fulfillment, c/o American Institute of Physics, 500 Sunnyside Blvd., Woodbury, NY 11797.

Visualizing nonlinear resonance in classical and quantum mechanics

Marshall Burns
President, Ennex Technology Marketing, Inc., Austin, Texas

(Received 22 October 1991; accepted 28 February 1992)

Results are shown of methods for representing the behavior of one-dimensional hydrogen perturbed by an electromagnetic wave. Different methods are used in classical and quantum mechanics. The quantum mechanical results appear to demonstrate the existence and overlap of resonance subspaces in Hilbert space, analogous to resonance zones in the classical phase space.

INTRODUCTION

The challenge of physics has always been to see patterns in the wash of data impinging on our senses all the time. While the quantity of data generated in experiments today is dramatically higher than ever before, computers allow us to manipulate those data much faster and more creatively, so that we can see patterns that would otherwise be hopelessly lost.

Nonlinear dynamics can be particularly frustrating because the irregular behavior it entails taunts us with its ostensible lack of any pattern. Yet diligent investigation by the pioneers of this field, taking advantage of the then-new tools of automatic computation, yielded amazing patterns in their data.[1] The much greater power and availability of today's computers further facilitates our search for regularity in the chaotic.

In this paper some results are shown of my work to see and understand the behavior of one of the simplest possible physical systems: a harmonically driven hydrogen atom. This system has attracted increased attention over the last 15 years because of its simplicity, its nonlinearity, and its yielding, under great experimental prowess of teams led by Bayfield and Koch, to observation.[2] While the classical simulations shown in this paper review previously understood results, the quantum mechanical simulations are new and demonstrate the existence of a quantal phenomenon corresponding to classical nonlinear resonance zones.

This Introduction mentions some of the computational tools used in performing the calculations. Then Sec. I describes the mathematical model underlying the calculations. Section II explains the meaning of *nonlinear resonace* in classical and quantum mechanics, including the phenomenon of *resonance zones*. Classical simulations demonstrating nonlinear resonance are shown in Secs. III ("physical" phase space) and IV (action-angle coordinates). The analogous quantum dynamics are shown in Sec. V. Finally, in Sec. VI the conclusions are drawn. In this paper, I focus on the computational and graphical aspects of my work. For more detail on other theoretical aspects and comparison with laboratory results, see Ref. 3.

The simulations were all performed by integrating the relevant equations of motion (Hamilton's equations for the classical cases, a linear system of Schrödinger's equations for the quantal) using a fourth-order Runge–Kutta algorithm implemented in C.[4] The numerical routines were compiled with the MicroSoft C Optimizing Compiler, Version 6.0 for running on an 80386-based microcomputer with an 80387 math coprocessor, and with the Cray Standard C Compiler for running on a Cray X-MP. The routines were written to be portable between the micro and the Cray, and to take advantage of vectorization on the Cray.

The graphics routines for the two-dimensional plots were also written in C and run on the microcomputer. The three-dimensional classical plots were generated by AcroBits AcroSpin, Version 2.0. For the classical simulations, the output was captured on the VGA screen by the Catch utility of LogiTech PaintShow Plus, Version 2.21, and stored in TIFF files. The color graphics for the quantal plots were output to a DataProducts P-132 color printer by a special driver written for this purpose.

I. THE HARMONICALLY DRIVEN STARK STATES OF HYDROGEN (HSH) MODEL

The complex behavior that makes hydrogen interesting arises under a perturbation that destroys a constant of its motion, changing it from an integrable system to quasi-integrable. An integrable system is one for which, in classical mechanics, the path in phase space is constrained to a subspace of dimensionality equal to the number of freedoms of the system. For example, the one-dimensional harmonic oscillator is integrable because its orbits in its phase space are ellipses (one-dimensional). Quasi-integrability means that the system has a control parameter and *appears* to be integrable under some range of values of this parameter, but shows itself nonintegrable when the parameter is changed. For example, in the case of the HSH system discussed below, the parameter is the electromagnetic field strength, F.

The perturbation considered here is a monochromat-

ic, linearly polarized, electromagnetic wave. The energy of interaction is just the scalar product of the electric vector of the wave with the dipole moment of the atom, so that the total system is modeled by (in atomic units, $m = e = 1$)

$$E = E_u + \mathbf{F}\cdot\mathbf{x}\cos(\omega t),$$

where E_u is energy of the unperturbed atom, $\mathbf{F}$ and ω are the peak field strength and angular frequency of the wave, and $\mathbf{x}$ is the separation vector of the proton and electron.

The laboratory experiments use excited states prepared by laser excitation in the presence of a static electric field. These are *extreme Stark* or *one-dimensional* states. In these states, the classical orbit or the quantum mechanical orbital of the electron lies almost along a straight line and the electron remains predominantly on one side of the proton. The electrostatic field is used only to prepare the initial states, and is not active in the region of the microwave perturbation. The polarization of the perturbing electromagnetic wave is lined up with the Stark axis of the atom. So the energy of the perturbed system can be modeled as

$$E = E_u + Fx\cos(\omega t) \quad \text{(HSH energy)}.$$

Thus the system to be studied is a hydrogen atom in an extreme Stark state, harmonically driven by a monochromatic, electromagnetic wave linearly polarized along the direction of the Stark stretching. This is the *harmonically driven Stark states of hydrogen*, or HSH, model.

For elongated, extreme Stark states, the appropriate coordinates for studying the hydrogen atom in quantum mechanics are the paraboloidal coordinates.[5] The one-dimensional approximation[6] is the special case $n_2 = m = 0$ in which the state function reduces to[7]

$$\langle \rho_1,\rho_2,\phi|n\rangle \approx \frac{1}{\sqrt{\pi}n^2} e^{-(\rho_1+\rho_2)/2n} L_n\left(\frac{\rho_1}{n}\right),$$

where $(\rho_1+\rho_2)/2$ is the radial distance, r, from the proton. This formula shows that the probability drops exponentially with r, except on the positive x axis, where ρ_2 is zero and the ρ_1 dependence of the Laguerre polynomial cancels the effect of the exponential. (On the negative x axis, ρ_1 is zero.) A plot of the absolute square of this function for $n = 40$ is shown in Fig. 1 (where the x axis is called "z"). This shows that the probability extends primarily along the positive x axis, and drops off rapidly everywhere else.

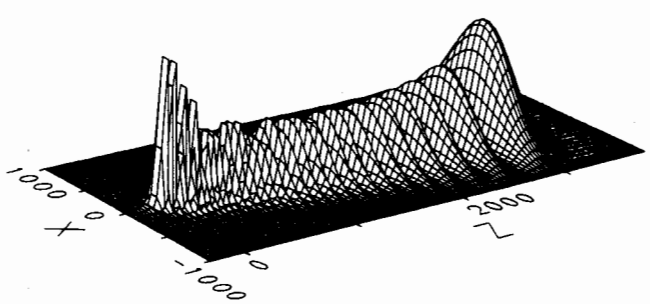

FIG. 1. Probability distribution for the extreme Stark state $|n_1,n_2,m\rangle = |39,0,0\rangle$, for which $n = 40$. [Fig. 1 from R. Blumel and U. Smilansky, Z. Phys. D **6**, 83 (1987)]. The z axis is this plot corresponds to what is called the x axis in the present paper.

II. LINEAR AND NONLINEAR RESONANCE IN CLASSICAL AND QUANTUM MECHANICS

In classical mechanics, a *linear* or *harmonic oscillator* can be defined in several ways, two of which involve a linearity: (i) A harmonic oscillator is a system with a linear restoring force, $F(x) = -k_F x$. (ii) A harmonic oscillator is a periodic system whose energy is linear in its action coordinate: $E = E_0 + k_E I$. Of these two definitions, it is the second that is more useful for explaining the phenomenon of *linear resonance*. Hamilton's equation for the angle coordinate says that the natural frequency of the system is independent of the action: $\omega = \partial E/\partial I = k_E$. This means that the dynamics of the system are unchanged by changes in the action values. If energy is absorbed from a perturbation with a frequency near ω, then that absorption can proceed without limit until there is a breakdown that alters the form of the energy.

In a *nonlinear oscillator*, the energy is a nonlinear function of the action, so the frequency does depend on the action: $\omega = \omega(I)$. Here, if the system has action I and is perturbed with a frequency near $\omega(I)$, then it exchanges energy with the perturbing system. But the resultant change in the value of the action changes also the value of the frequency ω. The system moves out of resonance, and so it does not keep exchanging energy indefinitely.

The behavior in classical linear resonance is a steady increase in the amplitude of oscillation, and a resultant migration of the system through regions of higher and higher energy in its phase space. The more complicated behavior in nonlinear resonance is characterized by the existence of *resonance zones* in the phase space. Inside each such zone, the system has a pronounced oscillatory response to the perturbation. At moderate perturbation strengths this response is localized within the zone with no migration from zone to zone. Moreover, whereas in a linear system the amplitude of the response is infinite at the exact resonant frequency, the amplitude of resonant oscillation at the center of each resonance zone is *zero*. Thus, at moderate perturbation strengths, the phenomenon of nonlinear resonance has an inherent *stability*.

As the strength of the perturbation is increased, however, the resonance zones grow in size and *overlap* each other. The boundaries delineating the zones, the *KAM surfaces*, are destroyed and the phase paths of the system wander from zone to zone. This migration is sensitively dependent on the initial conditions of the system, and is therefore *chaotic*. At moderate perturbation strengths, some KAM surfaces decay while others remain intact. The migration of the system is then restrained by the surviving KAM surfaces; the behavior is said to be *locally chaotic*. At higher and higher perturbation strengths, more and more KAM surfaces are destroyed. Eventually, the system becomes free to wander throughout its entire phase space, and the behavior is called *globally chaotic*.

There has been some doubt as to whether nonlinear resonance can occur in quantum mechanics. The objection is stated by pointing out that Schrödinger's equation is linear, so that there can be no nonlinear phenomena in quantum mechanics. This point of view is in error, however, because the linearity of Schrödinger's equation is linearity in the state vectors, and the significance of that linearity is that the space of quantum mechanical states is a linear (i.e.,

vector) space. What is relevant to the linearity of a resonance phenomenon is not the linearity of the equation of motion, but the linearity of the energy in the action coordinate.

There does not exist a pair of operators to correspond, in quantum mechanics, to the action and angle coordinates of classical mechanics.[8] However, in the classical limit, there is a correspondence between the index of the energy eigenvalues and the classical action. This suggests a way to carry over the concepts of linear and nonlinear resonance to quantum mechanics *in the special case of large energy quantum numbers*; that is, to consider linear resonance to occur in quantum mechanics when the energy eigenvalues of a system with a discrete energy spectrum form a linear function of their index: $E_n = E_0 + an$. The energy level spacing is then independent of the energy index: $E_{n+1} - E_n = a$. This means that the dynamics of the system are unchanged by changes in the energy level. If energy is absorbed in the form of photons of energy a, then that absorption can proceed without limit until there is a breakdown that alters the form of the energy. This is indeed the case for the quantum mechanical harmonic oscillator, whose energy eigenvalues are $E_n = \frac{1}{2}\hbar\omega + n\hbar\omega$.

With this understanding of quantum mechanical linear resonance, nonlinear resonance is understood to occur when the energy eigenvalues form a nonlinear function of their index, so the energy level spacing depends on the energy eigenvalue of the system: $E_{n+1} - E_n = a(n)$. If the system has energy E_n and is perturbed electromagnetically with a frequency $a(n)/\hbar$, then it exchanges photons with the perturbing system. But the resultant change in the energy level also changes the energy level spacing. The system moves out of resonance, and so it does not keep exchanging photons indefinitely.

The behavior in quantum mechanical *linear* resonance is a steady increase in the energy level of the system, similar to the situation in classical mechanics. But what is there in quantum mechanics to compare to the existence of *non*linear resonance zones in the phase spaces of classical mechanics? By studying an appropriate physical system on the border between classical and quantal behavior, extreme Stark states of hydrogen, the present work demonstrates the existence of resonance *subspaces* in the Hilbert space of the system (see Fig. 10). In a way that parallels the classical oscillatory behavior, the system undergoes a spreading of its probability within each zone. At moderate perturbation strengths the spreading is localized within the zone with no migration from zone to zone (Fig. 11). Thus, at moderate perturbation strengths, the phenomenon of nonlinear resonance has, also in quantum mechanics, an inherent *stability*. (There is, however, nothing to correspond to the zero amplitude of oscillation at the precise center of the classical resonance zone.)

As the strength of the perturbation is increased, the quantum mechanical resonance zones grow in size and overlap each other, just as in classical mechanics (Fig. 12). Since there are no phase paths, there is no parallel concept for sensitive dependence on initial conditions, and therefore no chaos in the quantum resonance picture. But the net result in the behavior is the same: the probabilistic spread of the system through a larger region of its space of states.

III. CLASSICAL HSH DYNAMICS IN THE PHYSICAL PHASE SPACE

The classical energy of the unperturbed one-dimensional hydrogen atom is, in atomic units ($m = e = 1$),

$$E_u = \frac{p^2}{2} - \frac{1}{x} = -\frac{1}{2I^2},$$

where the first form is in the "physical" coordinates of the motion, (x,p), and the second is in action-angle coordinates, (ξ,I). In physical coordinates, the motion of the electron is along an infinitesimally wide ellipse, whose foci coincide with the periapsis and apapsis of the orbit. The proton therefore lies *at* the periapsis of the orbit, and the apapsis is equal to the major axis of the ellipse, designated $2a$. Action-angle coordinates are discussed in Sec. IV; there the unperturbed motion is along a circle.

When the HSH perturbation is added to this energy in the physical coordinates:

$$E(x,p,t) = \frac{p^2}{2} - \frac{1}{x} + Fx\cos(\omega t),$$

at a frequency near that of the atomic motion, the effect is an oscillatory drift of the apapsis of the orbit, as shown in Fig. 2.

In oscillating within such regions, the orbits necessarily cross themselves. This means that the p-x space cannot be the phase space of this motion. The correct phase space is the four-dimensional, *extended* phase space,[9] in which the motion for each of the orbits shown above lies on a torus. If the ratio of the frequencies of the perturbation and the atomic motion is irrational, then the motion is aperiodic and fills the torus, as approximated in Fig. 3. If the ratio of frequencies is rational, then the motion is periodic, as shown in Fig. 4.

While the proper HSH phase space is four-dimensional, the most useful physical perspective comes from taking

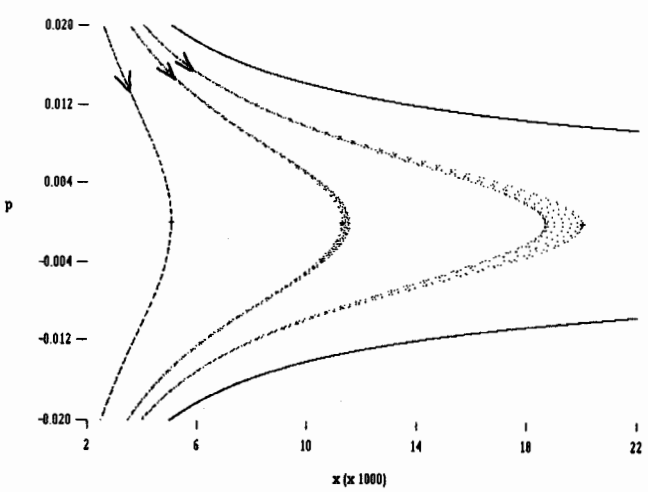

FIG. 2. Three orbits of the HSH atom viewed in the phase space of the unperturbed atom. The experimental parameters are $F = 1.947\times10^{-10}$ (1.000 V/cm) and $\omega = 1.509\times10^{-6}$ ($\nu = 9.923$ GHz). Each orbit oscillates within a region near its initial condition. The ionization boundary (orbit for $E = 0$) is also shown.

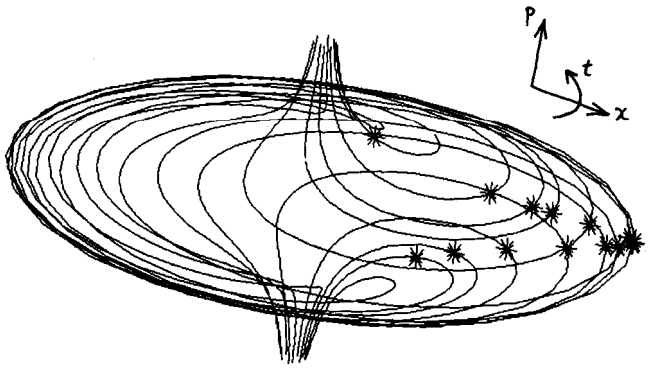

FIG. 3. The outermost orbit in Fig. 2, plotted in its energy subspace of the extended phase space. The orbit lies on a torus with no "donut hole," and with longitudinal circumferences extending to $p = \pm\infty$. The sense of motion is down at the top, spiraling around counterclockwise, and out through the bottom. The asterisks are those points lying in one copy of the original two-dimensional phase space; they are strobe points and form a Poincaré section of the orbit. This plot may be thought of as made by replotting the outermost orbit in Fig. 2 while rotating the two-dimensional phase space about its p axis, which becomes the central axis of the torus.

a two-dimensional slice through that space, known as a *Poincaré section*. This is made by strobing the motion at the frequency of the perturbation, and the results are shown in Fig. 5. The closed curves in this plot are the cross sections of families of *interstitial* tori growing in the midst of the original tori illustrated in Figs. 3 and 4. These interstitial tori wind around in between the original tori with various winding numbers, which are indicated by the labels in Fig. 5. The families of interstitial tori, represented in this figure by families of closed curves, are the resonance zones of the HSH system.

In addition to the regular orbits whose Poincaré sections are closed curves, there are also orbits whose evolution is chaotic and whose Poincaré sections consist of random scatterings of dots. This is caused by the overlap of the interstitial families of tori, i.e., by the overlap of resonance zones, as explained in Sec. II. Two such orbits are included in Fig. 5.

IV. CLASSICAL HSH DYNAMICS IN ACTION-ANGLE COORDINATES

The plots in Sec. III are made in the "physical" phase space of the unperturbed one-dimensional hydrogen atom, and in the extended phase space derived from that space. This section looks at the motion in the action-angle coordinates of the unperturbed atom. The action is

$$I \equiv \frac{1}{2\pi}\oint p\,dx = \sqrt{a} = \sqrt{-\frac{1}{2E_u}},$$

where a is the semimajor axis of the orbit ellipse, and E_u is the unperturbed energy.

The importance of the action-angle coordinates is the correspondence, for large values, between the action in classical mechanics and the principal quantum number, or energy index, in quantum mechanics.

In this coordinate system, the HSH energy has the form

$$E(\xi,I,t) = -\frac{1}{2I^2} + Fx(\xi)\cos(\omega t)$$

$$= -\frac{1}{2I^2} + \frac{FI^2}{2}\sum_{M=-\infty}^{\infty} A_M \cos(M\xi - \omega t),$$

where

$$\left\{ \begin{matrix} A_0 = -3 \\ A_{M\neq 0} = \dfrac{2J'_M(M)}{M} \end{matrix} \right\},$$

and $J'_M(z)$ is the first derivative of the Bessel function of the first kind, taken with respect to z and evaluated at z. The values of A_M for $M \in \{1,2,\ldots,5\}$ are 0.650, 0.224, 0.118, 0.0745, and 0.0520.

From this perspective the HSH perturbation takes the form of an infinite superposition of rotating cosine potentials, indexed by the integers, including a zeroth-order, standing cosine potential. The M th cosine potential in the series has amplitude $FI^2A_M/2$ and rotates (except for $M = 0$) with angular frequency ω/M. This frequency is either positive or negative (meaning an either counterclockwise or clockwise sense of rotation), according to the

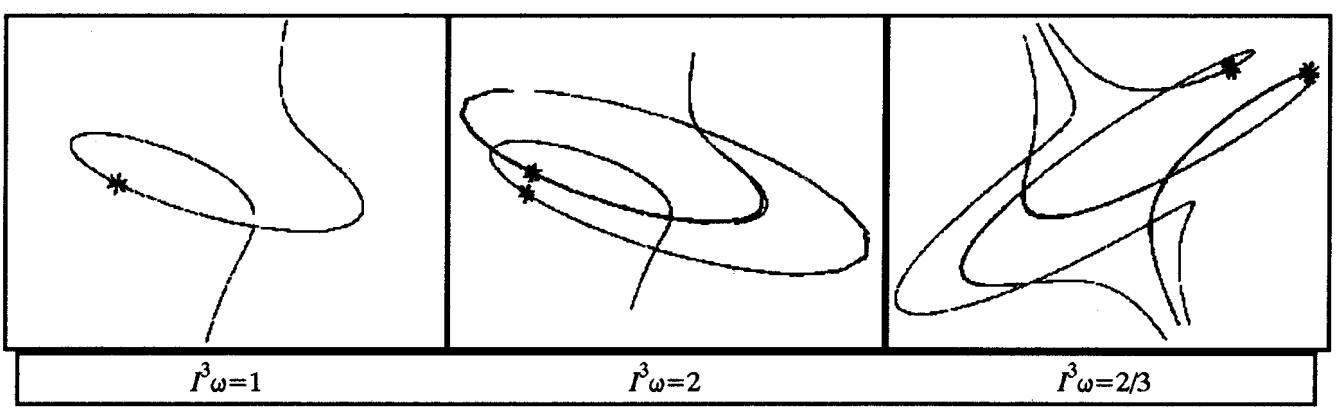

FIG. 4. Trajectories of the HSH atom in its energy subspace of the extended phase space, for three special cases where the ratio of frequencies is a rational number. The asterisks are strobe points, those points appearing when t is an integer multiple of the perturbation period, $2\pi/\omega$. Although each orbit appears to be a single curve spiraling around from top to bottom, each such curve is actually traversed several times in the calculation, showing that the motion is periodic. The different orientations of the p axes in the different plots is for visual purposes only, and is not physically significant.

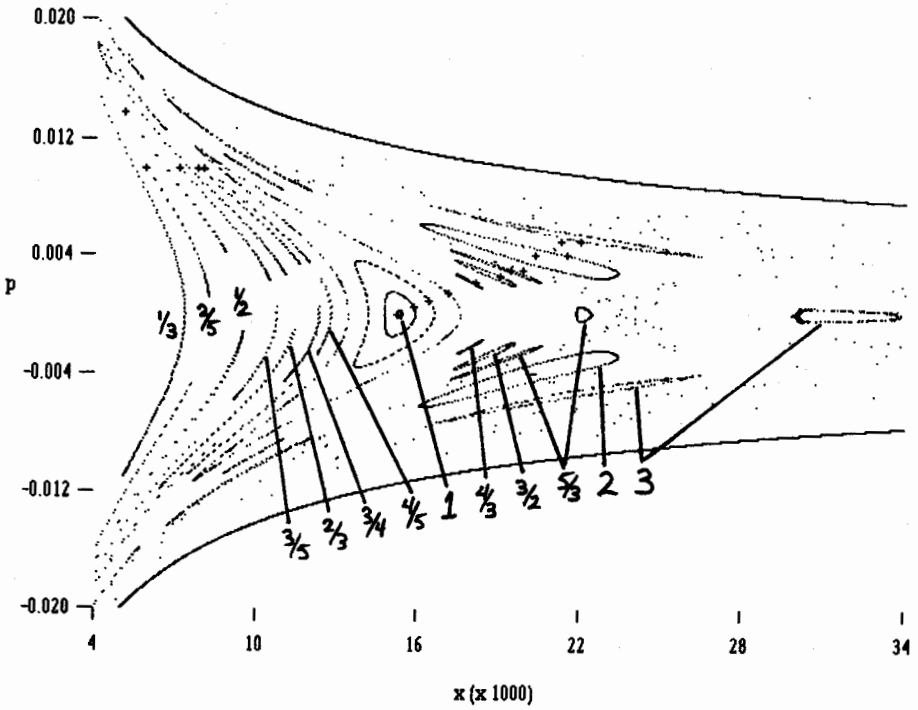

FIG. 5. Strobe plot of HSH phase paths for various initial conditions.The perturbing electromagnetic wave has peak field strength $F = 1.947 \times 10^{-10}$ (1.000 V/cm) and angular frequency $\omega = 1.509 \times 10^{-6}$ ($\nu = 9.923$ GHz). The fraction labeling each island chain indicates the winding number of the corresponding orbit on its torus. The outer curve is the ionization boundary (orbit for $E = 0$).

relative sign of M and ω. These rotating potentials can resonate with the underlying motion of the atom, which has angular frequency $d\xi/dt = 1/I^3$. The resonance condition is $I \approx (M/\omega)^{1/3}$ for some M.

If the HSH perturbation is weak enough, then in each resonance zone the effect of the perturbation is dominated by one particular term. In such a region the effective energy is

$$E^{(M)}(\xi,I,t) = -\frac{1}{2I^2} + \frac{FI^2 A_M}{2}\cos(M\xi - \omega t),$$

(singly resonant HSH energy).

This energy can be used to study the HSH dynamics under each individual term of its perturbation, independent of the others. The resonances arising from this energy are called *primary resonances*. The interactions of neighboring resonances lead again to an identical resonance structure. Structures arising from the interaction of two primaries are *secondary* resonances. Higher-order structures likewise appear.

Three ways of viewing the motion of a singly resonant HSH system are shown in Fig. 6, for the case $M = 2$. *The second primary resonance zone* is clearly visible in these plots.

The polar plots in Fig. 6, and also Fig. 7, use a graphic

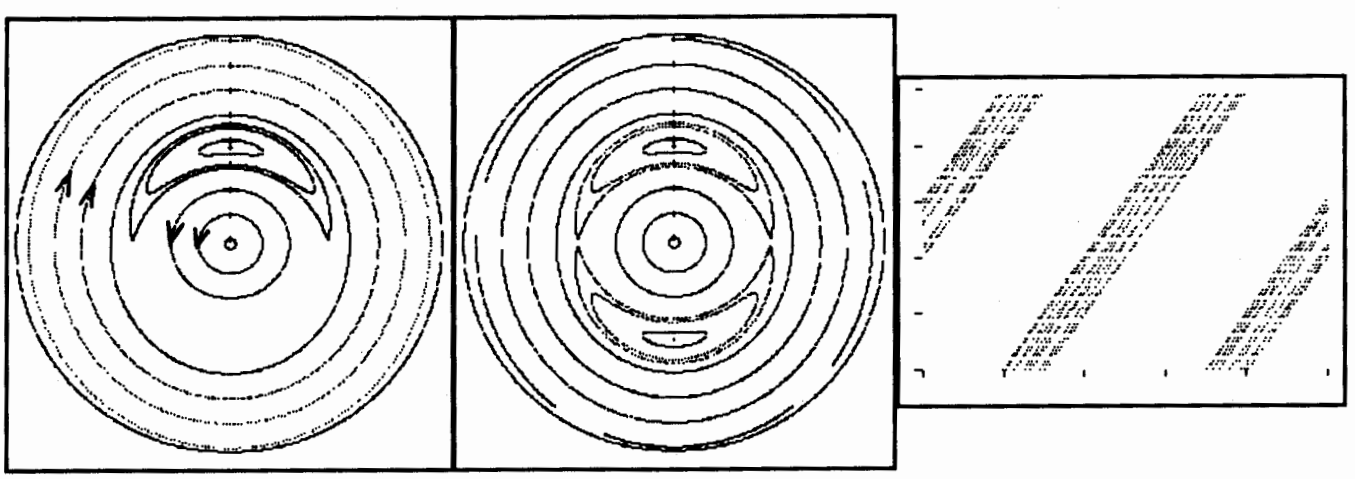

FIG. 6. Three views of the second primary HSH resonance zone, made by plotting the behavior of the singly resonant HSH system with $M = 2$ in three different spaces. On the left are shown phase paths in a frame of reference that is rotating along with the cosine potential, i.e., with angular frequency ω/M. In the center is a Poincaré section of the four-dimensional extended phase space, made by strobing the motion at the frequency of the perturbation, ω. The right-hand view uses the topological equivalence between a torus and a rectangle with opposite sides identified, and plots a single orbit in such a rectangle. The experimental parameters for all three plots are $F = 2 \times 10^{-10}$ (1.0 V/cm) and $\omega = 2\pi/(5 \times 10^6)$ ($\nu = 8.26$ GHz). In the two polar plots the range of the radial coordinate, the action, is $I \in (78,162)$. The rectangular plot covers $\xi \in (0,2\pi]$ horizontally and $t \in (0,5 \times 10^6]$ on the vertical axis.

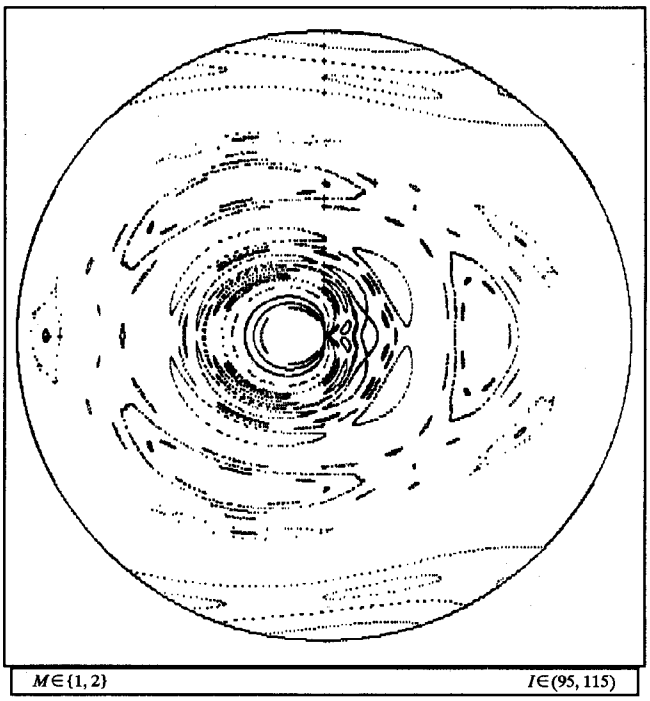

FIG. 7. Strobe plot of the doubly resonant HSH system for $M\in\{1,2\}$. The other parameters are the same as for Fig. 6. The region plotted is that between the first and second primary resonances. Several secondary and higher-order resonances are visible.

distortion to increase their useful area. Since the regions of interest, those where the resonance zones are located, have fairly high values of the action, the center of the (I,ξ) polar plane is of little interest. A (large) neighborhood of the origin is therefore deleted, which amounts to a magnification of the I scale of the data. For each polar plot, a range is given for the action values represented by the radial component of the graph. An orbit of constant action equal to the lower number in this range would appear as a single point at the center of the plot.

The HSH energy with two terms included in the perturbation,

$$E^{(M,N)}(\xi,I,t) = -\frac{1}{2I^2}+\frac{FI^2}{2}(A_M\cos(M\xi-\omega t) + A_N\cos(N\xi-\omega t)),$$

(doubly resonant HSH energy),

governs the behavior of the HSH system in a region of phase space in which there are two primary resonances near each other. This can be used to study the interaction of primary resonances to generate secondary and higher-order resonances. An example is shown in Fig. 7 for $M=1$, $N=2$. A great depth of structure is evident.

The structures seen here are Poincare sections of interstitial tori analogous to those seen in Figure 5 in the physical phase space. The winding numbers of the tori in this plot are reciprocal to those in the physical phase space.

V. QUANTUM DYNAMICS OF THE HSH ATOM

The energy eigenvalues of the unperturbed, bound, one-dimensional hydrogen atom are, in atomic units $(m=e=\hbar=1)$,

$$E_{u_n} = -1/2n^2 .$$

The level splitting for the atom is given by the Balmer formula:

$$E_{n+1}-E_n=\frac{1}{2}\left(\frac{1}{n^2}-\frac{1}{(n+1)^2}\right)\underset{n\to\infty}{\to}\frac{1}{n^3},$$

which, for large values of the principal quantum number, approaches the same form as the frequency of the orbital motion in classical action-angle coordinates, with $I\to n$.

The HSH energy is obtained by adding the perturbation of an electromagnetic wave polarized along the axis of the atom:

$$\hat{E}\,|n\rangle=\left[-\frac{1}{2n^2}+F\hat{x}\cos(\omega t)\right]|n\rangle .$$

After expressing the matrix elements of the separation operator, $\hat{x}$, in paraboloidal coordinates,[5] this becomes

$$\hat{E}\,|n\rangle = -\frac{1}{2n^2}|n\rangle+\frac{Fn^2}{4} \times\sum_{M\gg -n}^{\ll n}A_M(e^{i\omega t}|n+M\rangle+e^{-i\omega t}|n-M\rangle) .$$

In classical action-angle coordinates (Sec. IV), the energy of this system gives rise to resonance between the rotation of the unperturbed system and the rotation of a set of cosine potentials. In quantum mechanics, resonance is explained in terms of the splitting between energy levels. In the above energy, the kets $|n\pm M\rangle$ represent transitions up and down by M levels, where M is an integer much smaller in magnitude than n. The microwave perturbation is in resonance with the atom if its photon size is a multiple by some M of the level splitting of the atom. So the resonance condition is, for large n, $n^3\omega\approx M$, where $|M|\ll n$. This is identical to the resonance condition in the classical case, except that the classical theory does not put a limit on the magnitude of M.

As in classical action-angle coordinates, in order to study the behavior due to individual resonances and their interactions, the energy used in the computer calculations includes a single term or a selected set of terms from the resonance sum. The resulting simulations demonstrate a phenomenon very similar to the classical HSH behavior, in that there are regions of confinement of probability in the space of energy levels. (In quantum mechanics, a *region* in a parameter space, such as in the space of energy levels, corresponds to a *subspace* in Hilbert space.) Furthermore, these regions expand and merge as the strength of the HSH perturbation is increased, as do the resonance zones in the classical theory.

V(a). Graphical techniques and singly resonant system

The initial state given to the computer was a zero-phase, definite-energy state, i.e., a state in which the real part of the amplitude was 1 for one energy state, and in which the corresponding imaginary part as well as the amplitudes for

all other energy values were all zero. The number of energy states included in the integration was a monotonically increasing variable controlled by the program; in essence, the space of energy levels was programmed to expand in step with the spreading of probability. The probability distribution was saved at regular intervals, and various other diagnostic and metric data were also recorded by the program. The calculation would continue either for a preset number of intervals, or until the space of energy levels had ceased to expand (according to a programmed formula), so that the atom could be presumed to have reached a steady state.

A sample of the data output at a single time step is shown in Fig. 8. This shows the energy configuration of the atom at a particular time after the turn-on of the perturbation. A complete calculation consists of a sequence of many such frames.

The configuration shown in a single time frame may or may not be representative of the evolution of the atom. In order to understand what is going on, it is necessary to get a unified picture of the entire sequence of frames. The simplest way to do this is to plot the frames side by side in repeated rows on a page, as in a comic strip. This still makes it difficult to get the flavor of the motion. Another technique that was tried was to flash the sequence of frames on the computer screen in quick succession, so as to show the evolution of the atom as a movie in energy-probability space. This was a lot of fun, but the moment-by-moment fleeting of the image prevented the formation of an overall impression. Another problem with the movies was the difficulty of comparing two or several time series with each other.

A method was found for representing the entire evolution of an atom, from the turn-on of the perturbation through steady state, in a single, static picture. The technique is to use color to represent the magnitude of probability; this frees up one of the two dimensions on the plotting surface to be used to represent time. The result is called here an *evolution plot*, and is shown in Fig. 9. Any vertical slice through this figure contains the same information as the probability plot for one time frame, such as Fig. 8, although with much lower resolution, since there are only nine colors. This technique makes it possible to see many aspects of the motion that are not evident from inspecting a series of individual frames. It is also easy to compare numerous time series for different values of a variable parameter, such as initial state, and quickly observe the effect that the variation has on the motion.

In the evolution plot of Fig. 9, the probability is seen to spread out evenly, both above and below the initial state. After spreading out to fill the region from about $n = 69$ to 95, the probability stays in this region, yet with some oscillation in its structure. The region through which the probability spreads is identified as the first primary resonance zone.

Unfortunately, when one tries to make a comparison of a large number of time series, the evolution plots exhibit the same weakness as the representation by individual time frames. In order to really *see* evidence of the quantum resonance zones, it is necessary to further collapse a series of evolution plots into a single picture. As can be seen in Fig. 9, the essential features of the probability distribution remain fairly stable after steady state is reached, yet with some oscillation in time. This suggests that the essential information about a single evolution is preserved if the entire plot is collapsed by averaging the probabilities for each energy eigenvalue over the time after steady state is reached. This reduces each evolution plot to a vertical slice so that a series can be juxtaposed to form a new type of plot, in just the same way as the color representations of time frames are juxtaposed to make an evolution plot.

If the parameter that varies between the vertical slices is the initial state of the atom, the result is what is called here a *distribution plot*, with an example being Fig. 10. Both the vertical and horizontal axes are measured in the index of the energy eigenvalue. A value on the horizontal axis denotes the initial condition of one particular calculation. A value on the vertical axis denotes a possible state in the energy-index space of each calculation. The color of the plot at the intersection of these two values indicates the extent to which a calculation has predicted the spread of probability from the initial energy state to a state with the energy index indicated on the vertical axis.

In the distribution plot of Fig. 10, the first primary resonance zone shows up as a distinctive square pattern. The probability spreads out to fill the square area in a manner that is almost completely independent of the initial state of the atom.

This plot is a compact representation of a large amount of data. It comprises vertical slices for a time series for each of 181 initial states, with the probabilities in each slice being obtained by averaging over several hundred, and in many cases upward of 1000 time frames.

It may be asked if the information in the evolution and distribution plots might not be conveyed more simply (and less expensively) and with greater resolution in a three-dimensional relief plot, instead of in color. This was tried, but it was found that while relief plots are useful for smooth surfaces, they do not adequately represent data with sharp or clustered peaks and troughs because one peak can hide another nearby peak or trough, and a trough can hide the depth of another trough nearby.

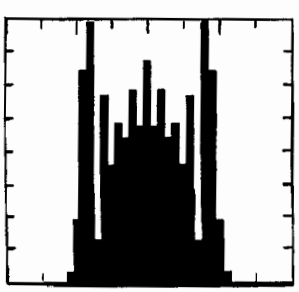

FIG. 8. Probability distribution of an approximation to the singly resonant HSH system with $M = 1$, $F = 0.95 \times 10^{-9}$ (4.9 V/cm), and $\omega = 80^{-3}$ ($\nu = 13$ GHz). The initial state is $n_0 = 80$; the state shown is for $t = 6.8 \times 10^6$ (1.6×10^{-10} sec). The horizontal axis is $n \in [60,100]$. The vertical axis is $P \in [0,0.08]$.

V(b). The doubly resonant HSH system in quantum mechanics

The significance of the resonance zones in classical mechanics is that their overlap is the route to chaotic behavior. So a very significant question is "Is there a quantum mechanical process analogous to the overlap of classical resonance zones?" This question is answered here in the

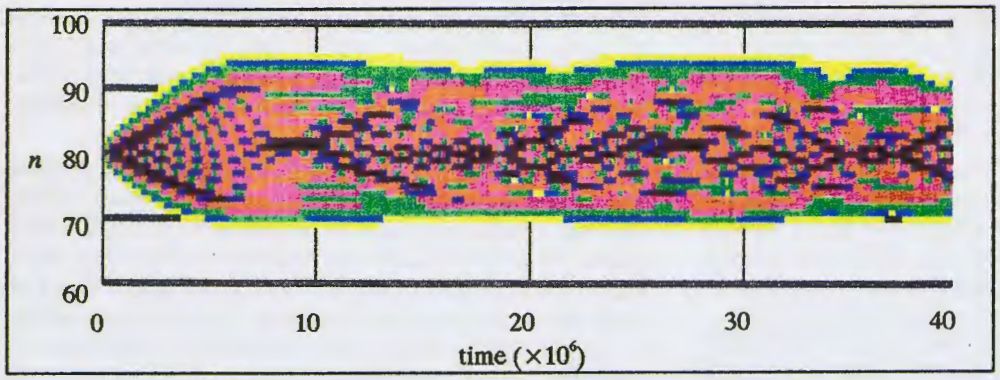

FIG. 9. Evolution plot for the singly resonant HSH system in quantum mechanics with $M = 1$ and $n_0 = 80$. The probability is seen to spread within a specific range of energy levels, and not beyond. This is the first primary resonance zone in quantum mechanics. The experimental parameters are $F = 0.95 \times 10^{-9}$ (4.9 V/cm) and $\omega = 80^{-3} = 1.9 \times 10^{-6}$ ($\nu = 13$ GHz).

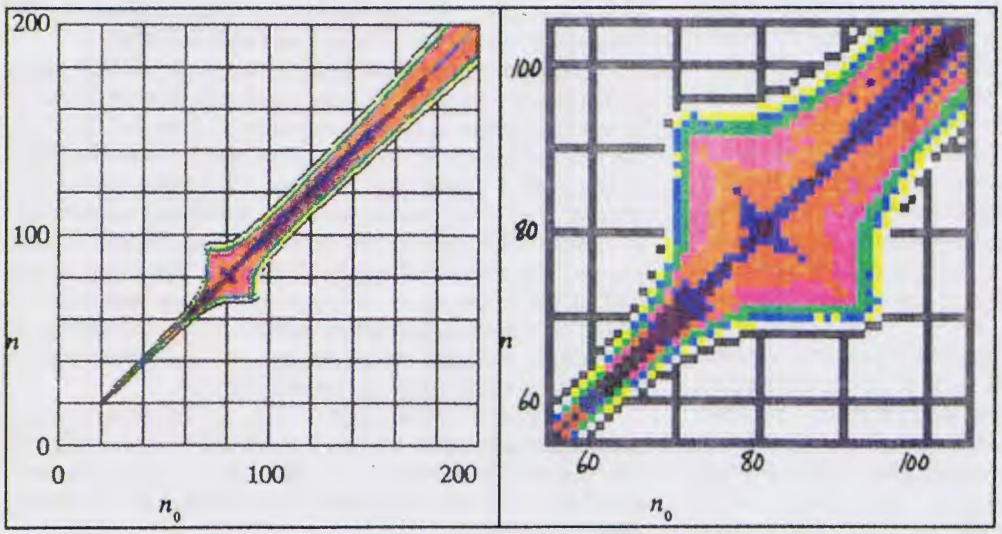

FIG. 10. Distribution plot for the singly resonant HSH atom with $M = 1$. On the left is shown the series of initial states from $n_0 = 20$–200. On the right is an expanded view of the vicinity of the resonance zone. This scheme of pairing a large scale plot with a closeup view of the resonance zone is used in all the distribution plots. The experimental parameters are the same as in Fig. 9.

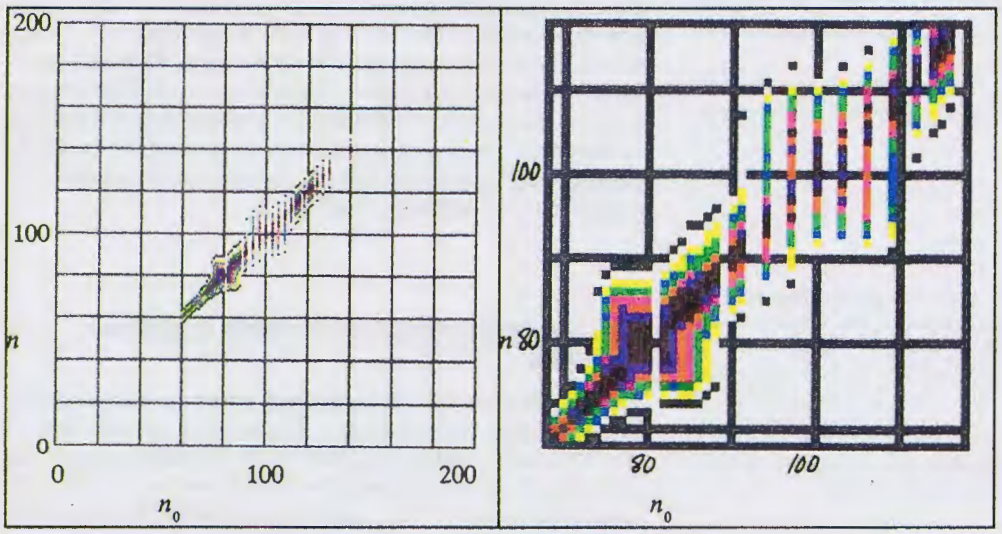

FIG. 11. Distribution plot for the doubly resonant HSH atom with $M \in \{1,2\}$, $F = 1.9 \times 10^{-10}$ (0.98 V/cm) and $\omega = 80^{-3} = 1.9 \times 10^{-6}$ ($\nu = 13$ GHz). The first and second primary resonance zones are visible.

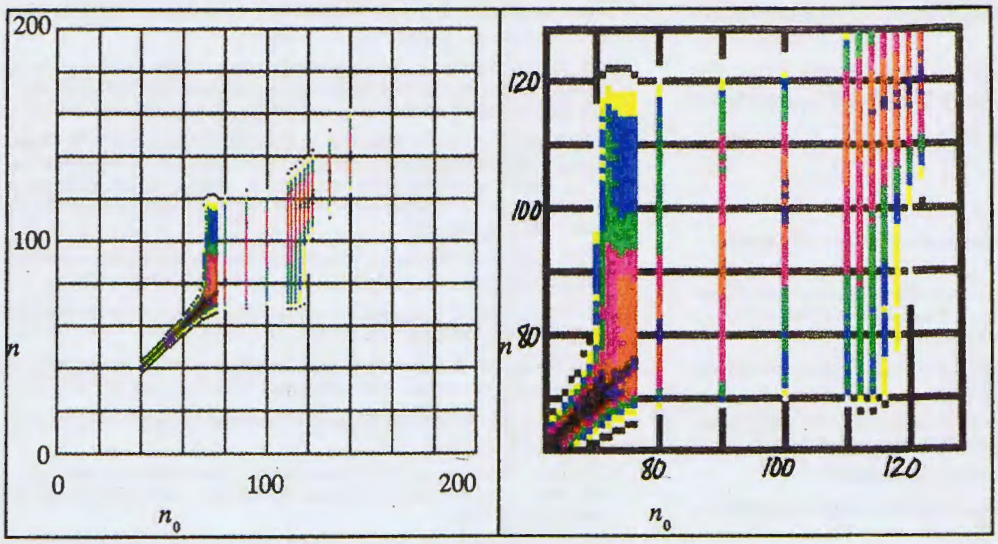

FIG. 12. Distribution plot for the doubly resonant HSH atom with $M\in\{1,2\}$, $F=0.95\times10^{-9}$ (4.9 V/cm) and $\omega=1.9\times10^{-6}$ ($\nu=13$ GHz). The first and second primary resonance zones have gone through overlap.

affirmative by demonstrating the overlap of neighboring quantum mechanical HSH resonance zones.

Unfortunately, the following distribution plots for combined resonances have vertical gaps in them because it was not practical to run simulations for all initial states. The calculation of a single, complete, distribution plot for an isolated resonance takes either several weeks on the very fast microcomputer used in this project, or a good part of a day on the Cray. The combined resonances run slower and thus take even more time. While the gaps make the plots harder to read than if all initial states were represented, the plots still show enough data to see the behavior of the resonance zones.

Figure 11 shows a distribution plot for the doubly resonant HSH system with $M\in\{1,2\}$. The microwave frequency is the same as is used in Fig. 10, but the field strength is reduced by a factor of 5. This figure shows unmistakable evidence of the first and second primary resonance zones. An atom starting in the region of one of these zones spreads in probability through that zone, and does not enter the other zone.

Figure 12 shows the result of restoring the field strength to the higher value. This plot shows a definite overlap of the resonance regions. The square area extends from about 70–120, which energy indices correspond to the lower edge of the first primary resonance zone and the upper edge of the second. For an initial state in either resonance zone, the probability spreads throughout both zones. In most parts, the probability still stays primarily in the original zone, with only very little spreading into the other zone. For $n_0=90$, however, which is midway between the locations of the two zones, the probability is fairly evenly spread out.

VI. CONCLUSIONS

In both classical and quantum mechanics, harmonically driven Stark states of hydrogen (HSH) exhibit nonlinear resonance between the orbital motion of the atom and the microwave perturbation. In classical mechanics, the resonance occurs when the angular frequency, in action-angle space, of the unperturbed atom is close to the frequency of one or more of an infinite number of rotating cosine potentials representing the perturbation. In quantum mechanics, resonance arises when the energy level spacing of the unperturbed atom is close to an integer multiple of the microwave photon size.

This resonance is manifested in the evolution of the atom by a structure of *resonance zones*, regions of stability in the space of states of the atom. The resonance zones grow with the strength of the HSH perturbation. As they grow, neighboring zones *overlap*, with the result that a system starting out in one zone is free to migrate within the larger total region of the overlapping zones. In classical mechanics this migration is by the evolution of the orbit; in quantum mechanics it is by the spreading of probability.

These results demonstrate that, despite totally different mathematical foundations, both classical and quantum mechanics do demonstrate the existence and overlap of resonance zones for this nonlinear system. In classical mechanics these are zones in the atom's phase space, and may be plotted in either the physical or action-angle coordinates. In quantum mechanics they are zones in the space of the atom's energy levels, which correspond to subspaces in its Hilbert space.

The ability to draw these conclusions comes directly from the ability, first to simulate the atom's behavior numerically, and second to manipulate the resulting data graphically. If we are willing to seek creative ways of representing our data, we have the opportunity to find the hidden patterns in what otherwise seems like an unmanageable mass of numbers.

ACKNOWLEDGMENTS

This paper is culled from my Ph.D. dissertation, accepted by the faculty of the University of Texas at Austin in April 1991. I wish to thank all of my colleagues at UT and other friends in Austin who made the pursuit and completion of this work possible. I also wish to thank all of the teachers in my life who showed me the way to this point. In particular, I am indebted to Professor Linda E. Reichl for her patient

guidance and stalwart confidence through five years of research.

Important financial support was received from the Welch Foundation of Texas, Grant No. F-1051, and from Ennex Technology Marketing, Inc.

REFERENCES

1. **The classic papers that demonstrated the power of computers to find patterns in nonlinear behavior are:**

E. Fermi, J. Pasta, and S. Ulam, "Studies of non linear problems," Los Alamos Document LA-1940, May 1955; reprinted in E. Fermi, *Collected Papers* (Univ. of Chicago, Chicago, IL, 1965), Vol. II, pp. 978–988

M. Henon and C. Heiles, "The applicability of the third integral of motion: Some numerical experiments," Astron. J. **69**, 73 (1964)

G. H. Walker and J. Ford, "Amplitude instability and ergodic behavior for conservative nonlinear oscillator systems," Phys. Rev. **188**, 416 (1969).

2. **The key papers in this expanding literature are experimental:**

J. E. Bayfield and P. M. Koch, "Multiphoton ionization of highly excited hydrogen atoms," Phys. Rev. Lett. **33**, 258 (1974)

J. E. Bayfield, L. D. Gardner, and P. M. Koch, "Observation of resonances in the microwave-stimulated multiphoton excitation and ionization of highly excited hydrogen atoms," Phys. Rev. Lett. **39**, 76 (1977)

P. M. Koch and D. R. Mariani, "Precise measurement of the static electric-field ionization rate for resolved hydrogen Stark substates," Phys. Rev. Lett. **46**, 1275 (1981)

J. E. Bayfield and L. A. Pinnaduwage, "Diffusionlike aspects of multiphoton absorption in electrically polarized highly excited hydrogen atoms," Phys. Rev. Lett. **54**, 313 (1985)

J. E. Bayfield and L. A. Pinnaduwage, "Microwave multiphoton n-decreasing transitions in electrically polarised [*sic*], highly excited hydrogen atoms," J. Phys. B **18**, L49 (1985)

K. A. H. van Leeuwen, G. v. Oppen, S. Renwick, J. B. Bowlin, P. M. Koch, R. V. Jensen, O. Rath, D. Richards, and J. G. Leopold, "Microwave ionization of hydrogen atoms: Experiment versus classical dynamics," Phys. Rev. Lett. **55**, 2231 (1985)

J. N. Bardsley, B. Sundaram, L. A. Pinnaduwage, and J. E. Bayfield, "Quantum dynamics for driven weakly bound electrons near the threshold for classical chaos," Phys. Rev. Lett. **56**, 1007 (1986)

P. M. Koch, K. A. H. van Leeuwen, O. Rath, D. Richards, and R. V. Jensen, "Microwave ionization of highly excited hydrogen atoms: experiment and theory," pp. 106–113 in *The Physics of Phase Space*, edited by H. Araki, J. Ehlers, K. Hepp, R. Kippenhahn, H. A. Weidenmuller, J. Wess, and J. Zittartz (Springer-Verlag, Berlin, 1987)

P. M. Koch, "Microwave ionization of highly-excited hydrogen atoms: A driven quantal system in the classically chaotic regime," pages 501–515 in *Electronic and Atomic Collisions, Invited Papers of the 15th International Conference on the Physics of*, Brighton, U.K., 87 07, edited by H. B. Gilbody, W. R. Newell, F. H. Read, and A. C. H. Smith (North-Holland, Amsterdam, 1988), pp. 22–28

E. J. Galvez, B. E. Sauer, L. Moorman, P. M. Koch, and D. Richards, "Microwave ionization of H atoms: Breakdown of classical dynamics for high frequencies," Phys. Rev. Lett. **61**, 2011 (1988)

and theoretical:

R. V. Jensen, "Stochastic ionization of surface-state electrons," Phys. Rev. Lett. **49**, 1365 (1982)

R. V. Jensen, 'Stochastic ionization of bound electrons," in *Chaotic Behavior in Quantum Systems*, edited by G. Casati (Plenum, New York, 1985), pp. 171–186

N. B. Delone, B. P. Krainov, and D. L. Shepelyanskii, "Highly-excited atoms in the electronmagnetic field," Usp. Fiz. Nauk. **26**, 551 (1983)

R. Blumel and U. Smilansky, "Quantum mechanical supperssion of classical stochasticity in the dynamics of periodically perturbed surface-state electrons," Phys. Rev. Lett. **52**, 137 (1984)

R. V. Jensen, "Stochastic ionization of surface-state electrons: Classical theory," Phys. Rev. A **30**, 386 (1984)

R. Blumel and U. Smilansky, "Suppression of classical stochasticity by quantum-mechanical effects in the dynamics of periodically perturbed surface-state electrons." Phys. Rev. A **30**, 1040 (1984)

R. Blumel and U. Smilansky, "Ionization of surface-state electrons by microwave fields: Quantum treatment," Phys. Rev. A **32**, 1900 (1985)

J. G. Leopold and D. Richards, "The effect of a resonant electric field on a one-dimensional classical hydrogen atom," J. Phys. B **18**, 3369 (1985)

J. G. Leopold and D. Richards, "The effect of a resonant electric field on a classical hydrogen atom," J. Phys. B **19**, 1125 (1986)

R. V. Jensen, "Stochastic ionization of highly excited hydrogen atoms." in *Oji International Seminar on Highly Excited States of Atoms and Molecules*, edited by S. S. Kano and M. Matsuzawa (Fuji-Yoshida, Japan, 1986), pp. 149–165

P. M. Koch, K. A. H. van Leeuwen, O. Rath, D. Richards, and R. V. Jensen, "Microwave ionization of highly excited hydrogen atoms: experiment and theory," in *The Physics of Phase Space*, edited by H. Araki, J. Ehlers, K. Hepp, R. Kippenhahn, H. A. Weidenmuller, J. Wess, and J. Zittartz (Springer-Verlag, Berlin, 1987), pp. 106–113

J. G. Leopold and D. Richards, "The effect of a combined static and microwave field on an excited hydrogen atom," J. Phys. B **20**, 2369 (1987)

R. V. Jensen, "Effects of classical resonances on the chaotic microwave ionization of highly excited hydrogen atoms," Phys. Scr. **35**, 668 (1987)

M. M. Sanders, R. V. Jensen, P. M. Koch, and K. A. H. van Leeuwen, "Chaotic ionization of highly excited hydrogen atoms," Nucl. Phys. B **2**, 578 (1987)

R. Blumel and U. Smilansky, "Microwave ionization of highly excited hydrogen atoms," Z. Phys. D **6**, 83 (1987)

G. Casati, I. Guarneri, and D. L. Shepelyansky, "Hydrogen atom in monochromatic field: Chaos and dynamic photon localization," IEEE J. Quantum Electron. **24**, 1420 (1988)

R. V. Jensen, S. M. Susskind, and M. M. Sanders, "Chaotic ionization of highly excited hydrogen atoms: comparison of classical and quantum theory with experiment," Phys. Rep. **201**, 1 (1991).

3. M. Burns, "Nonlinear resonance in the hydrogen atom," dissertation at University of Texas at Austin, May 1991

M. Burns and L. E. Reichl, "Nonlinear resonance in the hydrogen atom," Phys. Rev. A **45**, 333 (1992).

4. W. H. Press, B. P. Flannery, S. A. Teukolsky, and W. T. Vetterling, *Numerical Recipes in C, The Art of Scientific Computing* (Cambridge U.P., Cambridge, 1988).

5. L. D. Landau and E. M. Lifshitz, *Quantum Mechanics/Non-Relativistic Theory*, translated by J. B. Sykes and J. S. Bell (Pergamon, Oxford, 1977), 3rd ed., Sec. 37.

6. **The validity of the one-dimensional approximation is discussed in:**

D. L. Shepelyansky, "Quantum diffusion limitation at excitation of Rydberg atom in variable field," in *Chaotic Behavior in Quantum Systems*, edited by G. Casati (Plenum, New York, 1985), Sec. 2, pp. 187–204

R. Blumel and U. Smilansky, "Microwave ionization of highly excited hydrogen atoms," Z. Phys. D **6**, 83 (1987), Eq. (2.1)

J. N. Bardsley and B. Sundaram, "Microwave absorption by hydrogen atoms in high Rydberg states," Phys. Rev. A **32**, 689 (1985)

J. E. Bayfield and D. W. Sokol, "Excited atoms in strong microwaves: Classical resonances and localization in experimental final-state distributions," Phys. Rev. Lett. **61**, 2007 (1988)

R. V. Jensen, "Stochastic ionization of surface-state electrons: Classical theory," Phys. Rev. A **30**, 386 (1984).

7. M. Burns, "Nonlinear resonance in the hydrogen atom," dissertation at University of Texas at Austin, May 1991, Sec. D. 6.

8. **There is a literature of attempts to find such operators:**

W. Pauli, "The connection between spin and statistics," Phys. Rev. **58**, 716 (1940)

W. H. Furry, "Two notes on phase-integral methods," Phys. Rev. **71**, 360 (1947)

D. Judge and J. T. Lewis, "On the uncertainty relation for L_z and ϕ" and "On the commutator $[L_z,\phi]_-$,"Phys. Lett. **5**, 189 (1963), and Phys. Lett. **5**, 190 (1963)

W. H. Louisell, "Amplitude and phase uncertainty relations," Phys. Lett. **7**, 60 (1963)

L. Susskind and J. Glowgower, "Quantum Mechanical Phase and Time Operator," Physics **1**, 49 (1964)

E. R. Davidson, "On derivations of the uncertainty principle," J. Chem. Phys. **42**, 1461 (1965)

H. M. Kiefer and D. M. Fradkin, "Comments on separability operators, invariance ladder operators, and quantization of the Kepler problem in prolate-spheroidal coordinates," J. Mod. Phys. **9**, 627 (1968)

R. E. Peierls and J. N. Urbano, "The Villars formalism for nuclear rotation," Proc. Phys. Soc. **2-1**, 1 (1968)

E. C. Lerner, "Harmonic-oscillator phase operators," Nuovo Cimento B **56**, 183 (1968); and Nuovo Cimento B **57**, 1 (1968)

P. Carruthers and M. Martin Nieto, "Phase and angle variables in quantum mechanics," Rev. Mod. Phys. **40**, 411 (1986)

B. Leaf, "Canonical transformations and spectra of quantum operators," J. Mod. Phys. **10**, 1971 (1969)

B. Leaf, "Canonical operators for the simple harmonic oscillator," J. Mod. Phys. **10**, 1980 (1969)

E. C. Lerner, H. W. Huang, and G. E. Walters, "Some mathematical properties of oscillator phase operators," J. Mod. Phys. **11**, 1679 (1970)

J. J. Loeffel, A. Martin, B. Simon, and A. S. Wightman, "Pade approximants and the anharmonic oscillator," Phys. Lett. B **30**, 656 (1969)

J. C. Garrison and J. Wong, "Canonically conjugate pairs, uncertainty relations, and phase operators," J. Mod. Phys. **11**, 2242 (1970)

E. K. Ifantis, "Abstracts formulation of the quantum mechanical oscillator phase problem," J. Mod. Phys. **12**, 1021 (1971)

D. J. Simms, "Bohr-Sommerfeld Orbits and quantizable symplectic manifolds," Proc. Cambridge Philos. Soc. **73**, 489 (1973)

Y. Aharonov, E. C. Lerner, H. W. Huang, and J. M. Knight, "Oscillator phase states, thermal equilibrium and group representations," J. Mod. Phys. **14**, 746 (1973)

J. Dombrowski, "Spectral properties of phas operators," J. Mod. Phys. **15**, 576 (1974)

J-M. Levy-Leblond, "Who is afraid of nonhermitian operators? A quantum description of angle and phase," Ann. Phys. **101**, 319 (1976)

R. G. Newton, "Quantum action-angle variables for harmonic oscillators," Ann. Phys. **124**, 327 (1980)

R. A. Leacock and M. J. Padgett, "Hamilton-Jacobi/action-angle quantum mechanics," Phys. Rev. D **28**, 2491 (1983) [also Phys. Rev. Lett. **50**, 3 (1983)]

M. V. Berry, "Quantal phase factors accompanying adiabatic changes," Proc. Roy. Soc. London Ser. A **392**, 45 (1984)

M. V. Berry, "Classical adiabatic angles and quantal phase," J. Phys. A **18**, 15 (1985)

A. Galindo, "Phase and number," Lett. Math. Phys. **8**, 495 (1984)

J. H. Hannay, "Angle variable holonomy in adiabatic excursion of an integrable Hamiltonian," J. Phys. A **18**, 221 (1985)

Marshall Burns, "Discrete spectra and canonical conjugates," unpublished (1990).

9. A. J. Lichtenberg and M. A. Lieberman, *Regular and Stochastic Motion* (Springer-Verlag, New York, 1983), p. 14.